


Properties of the spin-liquid phase in the vicinity of the Lifshitz transition from Néel to spin-spiral state in frustrated magnets

Yaroslav A. Kharkov, Jaan Oitmaa, and Oleg P. Sushkov
School of Physics, University of New South Wales, Sydney 2052, Australia

 (Received 10 April 2018; revised manuscript received 17 September 2018; published 15 October 2018)

Three decades ago, Ioffe and Larkin pointed out a generic mechanism for the formation of a gapped spin liquid. In the case when a classical two-dimensional (2D) frustrated Heisenberg magnet undergoes a Lifshitz transition between a collinear Néel phase and a spin-spiral phase, quantum effects usually lead to the development of a spin-liquid phase sandwiched between the Néel and spin-spiral phases. In this work, using field theory techniques, we study properties of this universal spin-liquid phase. We examine the phase diagram near the Lifshitz point and calculate the positions of critical points, excitation spectra, and spin-spin correlation functions. We argue that the spin liquid in the vicinity of 2D Lifshitz point (LP) is similar to the gapped Haldane phase in integer-spin one-dimensional chains. We also consider a specific example of a frustrated system with the spiral-Néel LP, the J_1 - J_3 antiferromagnet on the square lattice that manifests the spin-liquid behavior. We present numerical series expansion calculations for this model and compare results of the calculations with predictions of the developed field theory.

DOI: [10.1103/PhysRevB.98.144420](https://doi.org/10.1103/PhysRevB.98.144420)

I. INTRODUCTION

Quantum spin liquids (SL) are “quantum disordered” ground states of spin systems, in which zero-point fluctuations are so strong that they prevent conventional magnetic long-range order. The main avenues towards realizing SL phases in magnetic systems are frustration and quantum phase transitions [1]. A particularly interesting example of SL is realized by tuning a frustrated magnetic system close to a Lifshitz point (LP) that separates collinear and spiral states. In the vicinity of the Lifshitz transition, the quantum fluctuations are strongly enhanced, resulting in a plethora of novel intermediate quantum phases [2].

A general argument in favor of a universal gapped SL phase near LP in two-dimensional frustrated Heisenberg antiferromagnets (AF) was first proposed by Ioffe and Larkin [3]. They showed that in the proximity of the LP quantum fluctuations destroy long-range spin correlations and create a region in the phase diagram with a finite magnetic correlation length. Subsequent studies found evidence for SL phases in various two-dimensional (2D) systems near the LP, including Heisenberg models on square and honeycomb lattices with second- and third-nearest-neighbor antiferromagnetic couplings [4–12]. However, the universality of the SL phase near LP, its ubiquitous properties, and the relation of the general argument to specific Heisenberg models has not previously been addressed.

In this paper we revisit the Ioffe-Larkin scenario and consider a field theory for a quantum Lifshitz transition between collinear and spiral phases in $D = 2 + 1$. Disregarding microscopic details of specific lattice models, we focus on the generic infrared physics at the LP. We develop a field-theoretic description of the $O(3)$ Lifshitz point based on the extended nonlinear sigma model. The nonlinear sigma model provides a unifying theoretical framework that allows us to analyze

the phase diagram, calculate positions of critical points, excitation spectra, and static spin-spin correlation functions. We demonstrate universal scalings of observables (gaps, position of critical points, etc.) in terms of the dimensionless SL gap at the LP, δ_0 , and show that the correlation length in the SL phase scales as $\xi \sim 1/\sqrt{\delta_0}$. We also argue that the LP spin liquid has a similarity to the gapped Haldane phase [13] in integer-spin one-dimensional (1D) chains. However, for the 2D SL there is no significant difference between the integer and half-integer spin cases.

A particular example of a system that has a Néel-spiral LP and hence manifests the spin-liquid behavior is the frustrated antiferromagnetic J_1 - J_2 - J_3 Heisenberg model on the square lattice with the second- and third-nearest-neighbor couplings as well as its simplified version, the J_1 - J_3 model. We perform numerical series expansion calculations for the J_1 - J_3 model and compare results of the calculations with predictions of the developed field theory.

The structure of the paper is as follows. In Sec. II we introduce the effective field theory describing the Néel to spin-spiral Lifshitz point. Section III addresses the quantum LP, quantum fluctuations, and the criterion for quantum “melting.” Next, in Sec. IV we calculate the spin-wave gap and positions of critical points. Section V addresses the static spin-spin correlator in the spin-liquid phase. In Sec. VI we describe our numerical series calculations for the J_1 - J_3 model with spin $S = \frac{1}{2}$ and 1 and compare results of these calculations with predictions of the field theory. Finally, our conclusions are presented in Sec. VII.

II. EFFECTIVE FIELD THEORY

We start with the following $O(3)$ symmetric Lagrangian describing a transition from the Néel to a spiral phase in

two-dimensional antiferromagnets:

$$\mathcal{L} = \frac{\chi_{\perp}}{2} (\partial_i n_{\mu})^2 - \frac{1}{2} n_{\mu} K(\partial_i) n_{\mu}, \quad (n_{\mu})^2 = 1. \quad (1)$$

Here, χ_{\perp} is the transverse magnetic susceptibility, n_{μ} is a unit length vector with $N = 3$ components corresponding to the staggered magnetization, ∂_i are the spatial gradients. The general form of the “elastic energy” operator $K(\partial_i)$ in inversion-symmetric systems reads as

$$K(\partial_i) = -\rho(\partial_i)^2 + \frac{b_1}{2}(\partial_x^4 + \partial_y^4) + b_2 \partial_x^2 \partial_y^2 + \mathcal{O}(\partial_i^6), \quad (2)$$

where we assume that the n field is sufficiently smooth. Classical limit of a quantum magnet corresponds to very large spin, $S \rightarrow \infty$. In terms of Lagrangian (1) this means that the time derivative term is negligible (zero). In this case, only the elastic energy (2) is relevant, and the spin stiffness ρ is the tuning parameter that drives the system across the Lifshitz transition. The spin stiffness is positive in the Néel phase, negative in the spiral phase, and vanishes at the Lifshitz point. The b terms containing higher-order spatial derivatives are necessary for stabilization of spiral order at negative ρ , and we will assume that $b_{1,2} > 0$. While the kinematic form of the Lagrangian (1) is dictated by global symmetries of the system, a formal derivation starting from a frustrated Heisenberg model can be found, e.g., in Ref. [3]. Note that in Lagrangian (1) we do not take into account topological terms. We will discuss their possible role later in the text.

The Lagrangian (1) can be applied to a number of models mentioned in the Introduction. Experimentally relevant system is an antiferromagnetic compound CaMn_2Sb_2 which consists of weakly coupled hexagonal layers [14]. This material accidentally lies very close to a Néel-spiral LP and the neutron scattering data [14] indicate some physics described by (1). We propose that another experimental possibility is related to rare-earth manganite materials $(\text{Tb}, \text{La}, \text{Dy})\text{MnO}_3$. These materials have layered structure with antiferromagnetically coupled layers. Due to the antiferromagnetic interlayer coupling, the dynamics of the system is described by the second-order time derivative as in usual antiferromagnets in agreement with Eq. (1) (see Ref. [15]), that makes the theory developed in this work applicable to manganites. Within each layer there are ferromagnetic nearest-neighbor and antiferromagnetic second-nearest-neighbor Heisenberg interactions leading to an in-plane frustration. Therefore, the intralayer structure can be commensurate (ferromagnetic), LaMnO_3 , or incommensurate spin spiral, TbMnO_3 and DyMnO_3 . Due to this reason, manganites could be tuned to the LP separating commensurate and incommensurate spin-spiral states by performing chemical substitution $\text{Tb}, \text{Dy} \rightarrow \text{La}$ or by applying external pressure. Of course, real compounds are three dimensional and contain many planes, however, thin films of these materials can manifest the LP physics considered in this paper. In the very end of Sec. VI, we discuss these materials.

In the AF phase of (1), $\rho > 0$, the rotational symmetry is spontaneously broken and the Néel vector has a nonzero expectation value, e.g., is directed along the z axis $\langle \mathbf{n} \rangle = \mathbf{e}_z$. In the spin-spiral phase, with $\rho < 0$, there is an incommensurate ordering

$$\mathbf{n}(\mathbf{r}) = \mathbf{e}_1 \cos(\mathbf{Q}\mathbf{r}) + \mathbf{e}_2 \sin(\mathbf{Q}\mathbf{r}), \quad (3)$$

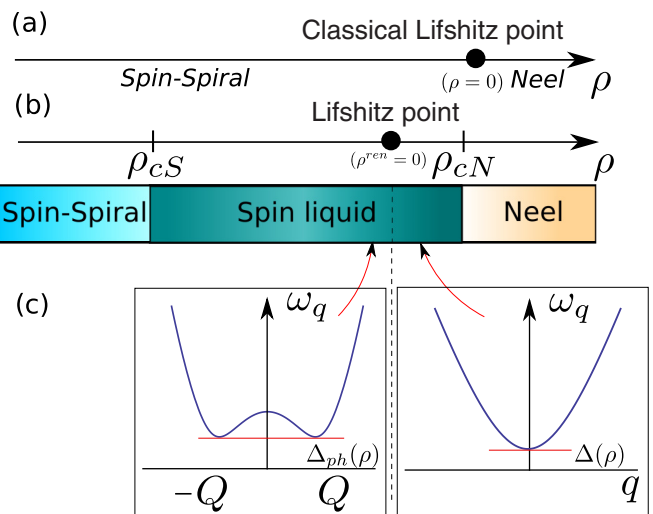


FIG. 1. Schematic phase diagram in the vicinity of the Lifshitz transition between collinear antiferromagnetic and spiral states: (a) classical Lifshitz transition ($S = \infty$), (b) quantum phase diagram; strong quantum fluctuations in the vicinity of the Lifshitz point result in the intermediate spin-liquid phase. (c) Excitation energy ω_q in the spin-liquid phase below and above LP.

where $\mathbf{e}_{1,2}$ are orthogonal unit vectors and \mathbf{Q} is the pitch of the spiral. For $b_1 \leq b_2$ the spiral wave vector is directed along x or y : $\mathbf{Q} = (\pm Q, 0), (0, \pm Q)$, where $Q^2 = |\rho|/b_2$. In the opposite case $b_1 > b_2$ the wave vector is directed along the main diagonals: $\mathbf{Q} = \frac{1}{\sqrt{2}}(\pm Q, \pm Q), \frac{1}{\sqrt{2}}(\pm Q, \mp Q)$, where $Q^2 = 2|\rho|/(b_1 + b_2)$. The relation between the coefficients b_1 and b_2 depends on the specific choice of the lattice model. In the “isotropic” case $b_1 = b_2$, the system has additional rotational degeneracy in the momentum space due to the arbitrary orientation of wave vector \mathbf{Q} . The additional degeneracy can destabilize spiral states and result in quantum spin-liquid states that have been predicted for three-dimensional (3D) antiferromagnets [16]. In this paper we will stay away from this special critical point. The classical phase diagram, $S = \infty$, is shown schematically in Fig. 1(a).

We would like to make a comment regarding Lagrangian (1). Parameters of any field theory depend on the momentum and energy scales. The dependence is described by renormalization group procedure. We assume that parameters in (1) and (2) are fixed at the ultraviolet cutoff $\Lambda \approx 1$, where unity corresponds to the inverse lattice spacing. Quantum fluctuations at scales larger than Λ but smaller than the boundary of magnetic Brillouin zone lead to a renormalization of the parameters $\rho \rightarrow \rho^{ren}, b_{1,2} \rightarrow b_{1,2}^{ren}, \dots$. Therefore, the values of the parameters in (1) and (2) can be different from those naively derived using spin-wave theory. As was pointed out by Ioffe and Larkin [3], this renormalization is especially relevant for the spin stiffness. The correction to the spin stiffness arises due to the b terms in (2). The easiest way to understand the correction is to consider the Néel phase and decompose the \mathbf{n} field into two transverse components and a longitudinal component:

$$\mathbf{n} = (\boldsymbol{\pi}, n_z), \quad n_z = \sqrt{1 - \boldsymbol{\pi}^2} \approx 1 - \boldsymbol{\pi}^2/2. \quad (4)$$

Hence, the following contribution from the b term arises:

$$\partial^2 n_z \partial^2 n_z \sim b (\partial^2 \boldsymbol{\pi}^2) (\partial^2 \boldsymbol{\pi}^2). \quad (5)$$

After appropriate averaging over quantum fluctuations, this term contributes to the spin stiffness. Following Polyakov [17] the field $\boldsymbol{\pi}$ can be decomposed into components with momenta smaller than Λ , $\boldsymbol{\pi}_<$, and a component with momenta larger than Λ , $\boldsymbol{\pi}_>$, $\boldsymbol{\pi} = \boldsymbol{\pi}_< + \boldsymbol{\pi}_>$. Substitution in (5) and averaging over high-energy fluctuations gives

$$b (\partial^2 \boldsymbol{\pi}^2) (\partial^2 \boldsymbol{\pi}^2) \rightarrow b (\partial \boldsymbol{\pi}_<)^2 ((\partial \boldsymbol{\pi}_>)^2) = \delta \rho_\Lambda (\partial \boldsymbol{\pi}_<)^2. \quad (6)$$

When averaging $(\partial^2 \boldsymbol{\pi}^2) \times (\partial^2 \boldsymbol{\pi}^2)$ each multiplier must contain the high- ($\boldsymbol{\pi}_>$) and the low- ($\boldsymbol{\pi}_<$) energy components. The terms originating from the averaging over the high-energy component in the b term with one multiplier containing only the high-energy and another only the low-energy components are total derivatives and therefore are irrelevant. Equation (6) demonstrates a positive correction to the spin stiffness. Therefore, quantum fluctuations always extend the Néel phase compared to the prediction of spin-wave theory that is indicated in Fig. 1(b). The Lifshitz point in the quantum case is shifted to the left compared to the Lifshitz point in the classical case. In the quantum case, the Lifshitz point is “buried” in the spin-liquid phase. Nevertheless, it is unambiguously defined as we discuss in the following sections.

III. QUANTUM LIFSHITZ POINT: THE PHASE DIAGRAM AND THE SPIN-LIQUID GAP

Quantum fluctuations destroy the classical Néel to spin-spiral Lifshitz transition [3]. Let us calculate local staggered magnetization n_z when approaching the LP from the Néel phase. Representing the staggered magnetization as $\langle n_z \rangle \approx 1 - \frac{1}{2} \langle \boldsymbol{\pi}^2 \rangle$, we obtain [18]

$$\begin{aligned} \langle \boldsymbol{\pi}^2 \rangle &\approx (N-1) \sum_q \int \frac{id\omega}{(2\pi)} \frac{1}{\chi_\perp \omega^2 - K(\mathbf{q}) + i0} \\ &= (N-1) \int \frac{d^2q}{(2\pi)^2} \frac{1/\chi_\perp}{2\omega_q}, \end{aligned} \quad (7)$$

where $\omega_q = \chi_\perp^{-1/2} \sqrt{\rho q^2 + b_1/2(q_x^4 + q_y^4) + b_2 q_x^2 q_y^2}$ and $N = 3$ is the number of components of \mathbf{n} field. In the vicinity of the LP, $\rho \rightarrow 0$, the integral (7) is logarithmically divergent, $\langle \boldsymbol{\pi}^2 \rangle \propto \ln(\frac{\Lambda}{\sqrt{\rho}})$, where Λ is the ultraviolet momentum cutoff. Hence, at some critical value of the spin stiffness $\rho = \rho_{cN}$ the staggered magnetization $\langle n_z \rangle$ vanishes, indicating a transition to the spin-liquid phase. In the spin-liquid phase, $\rho < \rho_{cN}$, a gap Δ must open to regularize the integral in Eq. (7):

$$\begin{aligned} \omega_q &\rightarrow \sqrt{\omega_q^2 + \Delta^2} \\ &= \sqrt{\Delta^2 + \chi_\perp^{-1} [\rho q^2 + b_1/2(q_x^4 + q_y^4) + b_2 q_x^2 q_y^2]}. \end{aligned} \quad (8)$$

Opening of the gap indicates an existence of a spin-liquid phase at which the long-range AF order is lost and the correlator $\langle \mathbf{n}(\mathbf{r}) \cdot \mathbf{n}(0) \rangle$ is exponentially decaying. Importantly, this is a generic gapped spin liquid originating from long-range fluctuations and is unrelated to a spin-dimer ordering. The SL gap is zero, $\Delta = 0$, at the critical point ρ_{cN} and the gap

increases when we proceed deeper into the spin-liquid phase. The SL phase stretches across a finite window $[\rho_{cS}, \rho_{cN}]$ in the vicinity of the LP, as depicted in Fig. 1(b).

The elementary spin excitations in the AF phase are two gapless Goldstone modes: transverse spin waves and a massive longitudinal (“Higgs”) mode [18]. Due to the unit length constraint ($\mathbf{n}^2 = 1$) the Higgs mode has a very large energy and can be disregarded. In the spiral phase there are three Goldstone modes: a sliding mode and two out-of-plane excitations. These three modes correspond to the three Euler angles defining the orientation of the $(\mathbf{e}_1, \mathbf{e}_2, \mathbf{e}_3)$ triad, where $\mathbf{e}_3 = [\mathbf{e}_1 \times \mathbf{e}_2]$ [15,19].

The excitation modes (8) in the SL phase are threefold degenerate due to $O(3)$ rotational invariance of the model. Above the LP ($\rho > 0$) the minimum of dispersion is located at $q = 0$, whereas below the LP ($\rho < 0$) the dispersion has four degenerate minima at the “spiral” wave vectors $q = \mathbf{Q}$. The evolution of the dispersion across the LP is schematically shown in Fig. 1(c). The change of the shape of the dispersion indicates the Lifshitz point.

The location of this critical point ρ_{cN} can be found by imposing the condition $\langle n_z \rangle \rightarrow 0$, which naively provides the following criterion for the transverse spin fluctuations $\langle \boldsymbol{\pi}^2 \rangle_c \approx 2$. This critical value for $\langle \boldsymbol{\pi}^2 \rangle$ is largely overestimated and it is not consistent with the unit length constraint. One can find a more accurate value of $\langle \boldsymbol{\pi}^2 \rangle_c$ by accounting for the next-order terms in the Taylor series expansion of $n_z = \sqrt{1 - \boldsymbol{\pi}^2}$ (see Appendix A), or alternatively by using the $1/N$ expansion for $O(N)$ nonlinear sigma model. The $1/N$ expansion has been extensively applied to describe quantum antiferromagnets. For the most relevant examples, see Refs. [20–22]. In the $1/N$ expansion approach we lift the hard constraint $\mathbf{n}^2 = 1$ by introducing a Lagrange multiplier

$$\mathcal{L} \rightarrow \mathcal{L} - \lambda(\mathbf{n}^2 - 1). \quad (9)$$

After integrating out the \mathbf{n} field in the new Lagrangian (9), we obtain an effective Lagrangian depending only on the auxiliary field λ :

$$\mathcal{L}_\lambda = N \text{tr} \ln[-\chi_\perp \partial_{tt} - K(\mathbf{q}) - \lambda] + \lambda. \quad (10)$$

We can find the saddle point in the Lagrangian \mathcal{L}_λ by calculating the variational derivative in (10) with respect to λ and regarding λ as a constant $\lambda = \chi_\perp \Delta^2$:

$$N \sum_q \int \frac{id\omega}{(2\pi)} \frac{1}{\chi_\perp (\omega^2 - \Delta^2) - K(\mathbf{q})} = 1. \quad (11)$$

The Lagrange multiplier in Eq. (11) has the meaning of the spin gap. Equation (11) determines the evolution of the gap $\Delta(\rho)$ with the spin stiffness in the SL phase. Comparing Eq. (11) with (7) we conclude that at the boundary between SL and AF phases $\langle \boldsymbol{\pi}^2 \rangle_c = (N-1)/N = \frac{2}{3}$. This criterion is quite natural for the $O(3)$ symmetric quantum critical point separating Néel and SL states. Nevertheless, this criterion underestimates $\langle \boldsymbol{\pi}^2 \rangle_c$. One can see this from the example of the $S = \frac{1}{2}$ 2D Heisenberg model on the square lattice. A textbook expression for the staggered magnetization is well

known [23]:

$$\langle n_z \rangle = 2\langle S_z \rangle = 1 - 2 \int_{\text{MBZ}} \frac{d^2q}{(2\pi)^2} \left(\frac{1}{\sqrt{1 - \gamma_q^2}} - 1 \right), \quad (12)$$

where $\gamma_q = \frac{1}{2}(\cos q_x + \cos q_y)$, and integration is performed over the magnetic Brillouin zone. In the limit $q < 1$, Eq. (12) is consistent with (7) since in this case $\chi_\perp = 1/8J$ and $\omega_q/J \approx \sqrt{2}q$, where J is the Heisenberg AF coupling. Integration over q in (12) gives a well-known result $\langle n_z \rangle \approx 2 \times 0.305$ which corresponds to $\langle \pi^2 \rangle \approx 0.78$ in the equation $\langle n_z \rangle \approx 1 - \frac{1}{2}\langle \pi^2 \rangle$. The integration in the corresponding long-wavelength approximation (7) with $N = 3$, $\chi_\perp = 1/8J$, $\omega_q \approx \sqrt{2}Jq$ and the ultraviolet cutoff $\Lambda = 1$ gives a close value $\langle \pi^2 \rangle \approx 0.89$. Both values are above $\frac{2}{3}$ and we know that the long-range AF order in the unfrustrated Heisenberg model still persists. Based on this analysis, we estimate the critical value of fluctuation as

$$\langle \pi^2 \rangle_c \approx 1, \quad (13)$$

which is an important result of this paper. Equation (13) is an analog of the Lindemann criterion [24] for quantum melting of long-range magnetic order in 2D quantum magnets. Our approach implicitly violates rotational invariance, but it allows us to calculate approximately the positions of critical points and the value of the spin-liquid gap.

The spin-liquid gap Δ is determined by Eqs. (7) and (8) from the condition $\langle \pi^2 \rangle = \langle \pi^2 \rangle_c \approx 1$. At $\rho > 0$ (the Néel side of LP), Δ coincides with the physical gap. On the spiral side of LP, $\rho < 0$, the physical gap corresponds to the excitation energy at the ‘‘spiral’’ wave vector \mathbf{Q} : $\Delta_{ph} = \min \omega_q = \sqrt{\Delta^2 + \frac{1}{\chi_\perp} K(\mathbf{Q})}$ [see Fig. 1(c)]. This gap is closed at the spin-spiral-SL critical point. Therefore, the position of this critical point ρ_{cS} is determined from the following two equations:

$$2 \sum_{q < \Lambda} \int \frac{id\omega}{(2\pi)} \frac{1}{\chi_\perp(\omega^2 - \Delta^2) - K(\mathbf{q}) + i0} = 1, \quad (14)$$

$$\Delta_{ph}^2 = \Delta^2 + \frac{1}{\chi_\perp} K(\mathbf{Q}) = 0.$$

At $\rho < \rho_{cS}$, the magnon Green’s function acquires a pole at imaginary frequency $\omega = \pm i\sqrt{|\Delta^2 + K(\mathbf{Q})/\chi_\perp|}$. This is the indication of an instability of the SL phase towards condensation of a static spiral with the wave vector \mathbf{Q} .

It is instructive to draw an analogy between the SL physics at 2D Lifshitz point and the one-dimensional Haldane spin chain. A condition similar to (11) determines the value of the Haldane gap [22]. Indeed, the integer spin- S Heisenberg model in the continuous limit can be mapped to the $O(3)$ relativistic nonlinear sigma model in $D = 1 + 1$ [13]. The model parameters are the speed of the magnon, $c = \sqrt{\rho/\chi_\perp} = 2JS$, and the transverse magnetic susceptibility, $\chi_\perp = 1/4J$ (J is the Heisenberg coupling constant). Proceeding by analogy with (7), we find the fluctuations of the spin in the Haldane model

$$\langle \pi^2 \rangle_c = 2 \int_0^\Lambda \frac{dq}{2\pi} \frac{1}{2\chi_\perp \sqrt{c^2 q^2 + \Delta^2}} \approx \frac{1}{2\pi c \chi_\perp} \ln \frac{c\Lambda}{\Delta}. \quad (15)$$

As we already discussed, the ultraviolet cutoff is $\Lambda \approx 1$. The logarithmically divergent $\langle \pi^2 \rangle$ in the Haldane model is analogous to the log-divergence in (7) at the LP. Numerical values of the Haldane gaps for $S = 1$ and 2 are known from density matrix renormalization group (DMRG) calculations: see, e.g., Ref. [25], $\Delta_{S=1}/J \approx 0.41$, $\Delta_{S=2}/J \approx 0.08$. Taking these values of the gap (15) we obtain the following critical values of fluctuations: $\langle \pi^2 \rangle_c \approx 0.5$ (for $S = 1$) and $\langle \pi^2 \rangle_c \approx 0.6$ (for $S = 2$), which are smaller than (13). We believe that the difference is due to different dimensionality. While DMRG is more reliable, it is interesting to note that the renormalization group analysis [22] for the integer spin Haldane chain gives $\langle \pi^2 \rangle_c = 1$.

The differences in the values of $\langle \pi^2 \rangle_c$ are not crucial when making comparisons between 1D and 2D systems. However, it is well known that properties of the spin chains with half-integer and integer spins are very different. The gapped SL phase in 1D appears only in the integer spin chains, while in contrast the excitations of half-integer spin chains are gapless spinons in agreement with the Lieb-Shultz-Mattis theorem [26]. We believe that the 2D spin liquid in the vicinity of LP point is generic and independent of the value of the lattice spin, the spin of quasiparticle is $S = 1$. The Lieb-Shultz-Mattis theorem states that in systems with half-integer spin per unit lattice cell and full rotational $SU(2)$ symmetry, the excitations are gapless or otherwise the ground state of the system is degenerate. The theorem was initially formulated for $D = 1 + 1$ systems and later generalized for higher spatial dimensions [27]. Technically, in $D = 1 + 1$ the dramatic difference between integer and half-integer spin is due to the topological Berry phase term which is not included in the Lagrangian (1) [13]. Topological effects in $D = 2 + 1$ correspond to skyrmions or merons [28].

In principle, topological configurations become more important when approaching the Lifshitz point [29]. However, such topological solutions are unstable within the model (1). Using scaling arguments one can see that due to the fourth spatial derivative term in the Lagrangian (1), the energy of localized skyrmions at LP behaves as $\sim b_{1,2}/R^2$, where R is the skyrmion radius. Therefore, any localized skyrmions energetically prefer to have large size $R \rightarrow \infty$ and only contribute to the boundary terms. Although the topological solutions might play a role to reconcile with the Lieb-Shultz-Mattis theorem, these configurations are statistically irrelevant in the bulk.

IV. SPIN-LIQUID EXCITATION GAP AND POSITIONS OF NÉEL-SPIN-LIQUID AND SPIN-SPIRAL-SPIN-LIQUID CRITICAL POINTS

In this section we calculate the excitation gap in the spin-liquid phase and positions of critical points separating different phases. The critical point separating the spin-liquid and the spin-spiral phases is calculated by two different methods: (i) approaching the point from the spin-liquid side, and (ii) approaching the point from the spin-spiral side.

In order to make our calculations more specific and having in mind comparison with the J_1 - J_3 model, in this section we set $b_2 = 0$. It is convenient to introduce dimensionless spin

stiffness and dimensionless gap parameters

$$\bar{\rho} = \frac{2\rho}{b_1}, \quad \delta = \sqrt{\frac{2\chi_{\perp}}{b_1}} \Delta. \quad (16)$$

At negative ρ the spiral wave vector is directed along the main diagonals $\mathbf{Q} = \frac{1}{\sqrt{2}}(Q, \pm Q)$:

$$Q^2 = |\bar{\rho}|. \quad (17)$$

In this section we calculate positions of the critical points and the spin-liquid gap expressed in terms of dimensionless gap $\delta_0 = \delta(\rho = 0)$ at the LP since it is a natural scaling parameter in the problem. In the limit $\delta_0 \ll 1$, all physical observables depend only on $\bar{\rho}$ and δ_0 .

A. Spin-liquid phase

First, we perform the analysis in the spin-liquid phase where $\delta \neq 0$. As we already discussed in Sec. III, the condition of criticality reads as

$$\langle \pi^2 \rangle_c \approx 1 \approx \frac{\sqrt{2}}{(4\pi^2)\sqrt{\chi_{\perp}b_1}} \int \frac{d^2q}{\sqrt{\bar{\rho}q^2 + q_x^4 + q_y^4 + \delta^2}}. \quad (18)$$

Let us determine the gap exactly at the LP. For $\delta_0 \ll 1$ the solution of (18) is

$$\delta_0 = 1.7\Lambda^2 e^{-\frac{2\sqrt{2}\pi}{\zeta}\sqrt{\chi_{\perp}b_1}}. \quad (19)$$

The constant ζ in the exponent is given by the angular part of the q integral $\zeta = \frac{2}{\pi}K(\frac{1}{2}[1 - \frac{b_2}{b_1}])$, where $K(m) = \int_0^{\pi/2} d\phi \frac{1}{\sqrt{1-m\sin^2\phi}}$ is the complete elliptic integral. In the specific case under consideration, $b_2 = 0$, $\zeta = \frac{2}{\pi}K(1/2) \approx 1.18$. The numerical prefactor $A = 1.7$ in (19) is found by performing a least-squares fitting of the integral in Eq. (18). While Eq. (19) is derived for $\delta_0 \ll 1$, however, direct numerical integration in (18) shows that (19) practically works up to $\delta_0 \leq 0.6-0.7$.

In order to determine the position of the Néel critical point ρ_{cN} , we evaluate the integral in (18) at $\delta \ll \bar{\rho} \ll 1$:

$$\frac{1}{2\pi} \int \frac{d^2q}{\sqrt{\bar{\rho}q^2 + q_x^4 + q_y^4 + \delta^2}} \approx \frac{\zeta}{2} \ln\left(\frac{2.9\Lambda^2}{\bar{\rho}}\right) - \frac{\delta}{\bar{\rho}}. \quad (20)$$

The condition $\delta = 0$ gives the position of the Néel-SL critical point $\bar{\rho}_{cN}$:

$$\bar{\rho}_{cN} \approx 2.9\Lambda^2 e^{-\frac{2\sqrt{2}\pi}{\zeta}\sqrt{\chi_{\perp}b_1}} \approx 1.65\delta_0. \quad (21)$$

According to (20) in the vicinity of the Néel-SL critical point $\bar{\rho} < \bar{\rho}_{cN}$, the gap grows linearly as $\delta \approx 0.64(\bar{\rho}_{cN} - \bar{\rho})$, that corresponds to a mean-field prediction.

The spin stiffness ρ_{cN} at the transition point from the Néel phase to the spin-liquid phase is small but still finite. Therefore, we believe that the transition belongs to the standard $O(3)$ universality class, the same as that in the bilayer quantum antiferromagnet (see, e.g., Ref. [30]). The correct critical index for $O(3)$ transition is $\nu \approx 0.7$, which implies $\delta \propto (\bar{\rho}_{cN} - \bar{\rho})^{\nu}$.

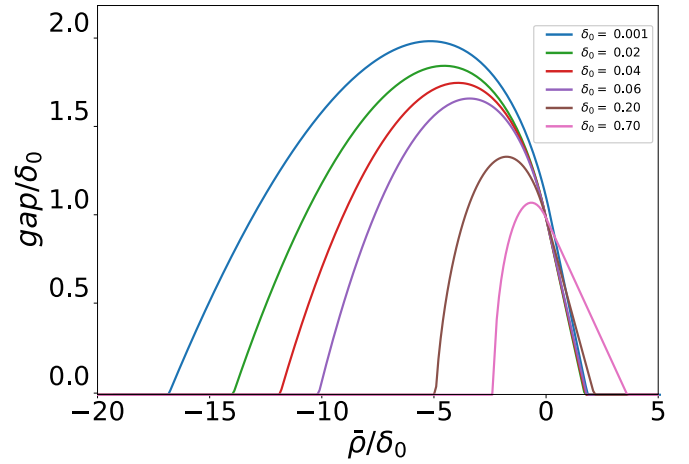


FIG. 2. Dimensionless SL gap, where $\text{gap} = \delta$ for $\rho > 0$ and $\text{gap} = \alpha$ for $\rho < 0$, versus spin stiffness for different values of δ_0 .

On the side of negative spin stiffness $\bar{\rho}_{cS} < \bar{\rho} < 0$, the dimensionless physical gap reads as

$$\alpha = \sqrt{\frac{2\chi_{\perp}}{b_1}} \Delta_{ph} = \sqrt{\delta^2 - \bar{\rho}^2/2}. \quad (22)$$

The condition $\alpha = 0$ determines the position of the spin-spiral to SL critical point ρ_{cS} . Calculating the integral in (18) at $\alpha \ll Q^2 \ll 1$ we find

$$\begin{aligned} & \frac{1}{2\pi} \int \frac{d^2q}{\sqrt{Q^4/2 - Q^2q^2 + q_x^4 + q_y^4 + \alpha^2}} \\ & \approx \zeta \ln\left(\frac{5.4\Lambda}{Q}\right) - 2\frac{\alpha}{Q^2}. \end{aligned} \quad (23)$$

The condition $\alpha = 0$ gives the position of the critical point $\bar{\rho}_{cS}$:

$$\bar{\rho}_{cS} = -Q^2 \approx -17\delta_0. \quad (24)$$

The gap in the vicinity of this critical point is $\alpha = 0.27(\bar{\rho} - \bar{\rho}_{cS})$. This is a mean-field result and we believe that the transition at ρ_{cS} does not belong to a standard universality class.

The dimensionless gap found by numerical solution of Eq. (18) for different values of δ_0 in the entire SL region $\rho_{cS} < \rho < \rho_{cN}$ is presented in Fig. 2. From this figure we conclude that asymptotic solutions given by Eqs. (21) and (24) become valid only at sufficiently small values of δ_0 (i.e., large values of S): Eq. (21) is valid at $\delta_0 \lesssim 0.2$ and Eq. (24) is valid only for very small gaps $\delta_0 \lesssim 0.02$. The asymmetry between ρ_{cS} and ρ_{cN} evident from Fig. 2 is due to stronger quantum fluctuations in the spiral ($\rho < 0$) region compared to the $\rho > 0$ domain.

B. Spin-spiral phase

An alternative method to determine $\bar{\rho}_{cS}$ is to approach the spiral-SL critical point from the spiral phase and find the condition when quantum fluctuations melt the spiral. This method does not allow us to access the spin-liquid phase, but it allows to find $\bar{\rho}_{cS}$.

The fluctuations of spiral consisting of the out-of-plane $h(\mathbf{r}, t)$ and in-plane modes $\phi(\mathbf{r}, t)$ can be parametrized in the form

$$\vec{n} = (\sqrt{1-h^2} \cos(\mathbf{Q} \cdot \mathbf{r} + \phi), \sqrt{1-h^2} \sin(\mathbf{Q} \cdot \mathbf{r} + \phi), h). \quad (25)$$

The total quantum fluctuation orthogonal to the spin alignment in the spiral state reads as

$$\begin{aligned} \langle \pi^2 \rangle &= \langle \phi^2 \rangle + \langle h^2 \rangle, \\ \langle \phi^2 \rangle &= \frac{1}{(4\pi^2)\sqrt{2}\chi_{\perp}b_1} \int \frac{d^2q}{\sqrt{2Q^2q^2 + q_x^4 + q_y^4}}, \\ \langle h^2 \rangle &= \frac{1}{(4\pi^2)\sqrt{2}\chi_{\perp}b_1} \int \frac{d^2q}{\sqrt{Q^4/2 - Q^2q^2 + q_x^4 + q_y^4}}. \end{aligned} \quad (26)$$

The denominators in the integrals for $\langle \phi^2 \rangle$ and $\langle h^2 \rangle$ in (26) represent the dispersions for the Nambu-Goldstone excitations: the sliding mode and the out-of-plane mode (see details in Appendix B). Evaluating the integrals with logarithmic accuracy, we obtain

$$\langle \pi^2 \rangle \approx \frac{1}{(2\pi)\sqrt{2}\sqrt{\chi_{\perp}b_1}} \zeta \ln \left(\frac{6.5\Lambda^2}{Q^2} \right). \quad (27)$$

Now, applying the same criterion for the critical point $(\pi^2)_c \approx 1$, we find the critical $\bar{\rho}_{cS}$ in the limit of $\delta_0 \ll 1$:

$$\bar{\rho}_{cS} \approx -6.5\Lambda^2 e^{-\frac{2\sqrt{2}\pi}{\zeta} \sqrt{\chi_{\perp}b_1}} \approx -4\delta_0. \quad (28)$$

The central point of this section is to demonstrate that exponents in Eqs. (24) and (28) are identical. This is a necessary test of validity of the calculation with logarithmic accuracy. However, the prefactor calculated in the spin-liquid phase [Eq. (24)] is different from that calculated in the spin-spiral state [Eq. (28)]. This emphasizes the fact that our calculation is only approximate. Practically this disagreement is not significant. We already pointed out that Eq. (24) is valid only for extremely small gaps, $\delta_0 \lesssim 0.02$. At larger values of δ_0 the position of the critical point ρ_{cS} is different from (24). From Fig. 2 one finds $\bar{\rho}_{cS} = -10\delta_0$ at $\delta_0 = 0.06$; $\bar{\rho}_{cS} = -5\delta_0$ at $\delta_0 = 0.2$; $\bar{\rho}_{cS} = -2.5\delta_0$ at $\delta_0 = 0.7$. These values are very different from the asymptotic equation (24). When approaching from the spin-spiral phase, numerical evaluation of (26) combined with the criticality condition (13) gives the following critical points: $\bar{\rho}_{cS} = -3.7\delta_0$ at $\delta_0 = 0.06$; $\bar{\rho}_{cS} = -3.6\delta_0$ at $\delta_0 = 0.2$; $\bar{\rho}_{cS} = -2.2\delta_0$ at $\delta_0 = 0.7$. Again, this is different from the asymptotic $\delta_0 \rightarrow 0$ [Eq. (28)]. Importantly, for the practically interesting case of J_1 - J_3 model which we consider in Sec. VI, where $\delta_0 > 0.15$, the both methods give close positions of the critical point.

As was mentioned in Sec. II in the presence of in-plane rotational symmetry $b_1 = b_2$ (e.g., frustrated Heisenberg model on the hexagonal lattice), quantum fluctuations become especially strong. In fact, when approaching the critical point ρ_{cS} the integral $\int_q \frac{1}{\sqrt{\Delta^2 + K(q)}} \propto \int_q \frac{1}{\sqrt{\alpha^2 + (q^2 - Q^2)^2}}$ is logarithmically divergent for $\alpha \rightarrow 0$ at $q = Q$. It implies that one has to

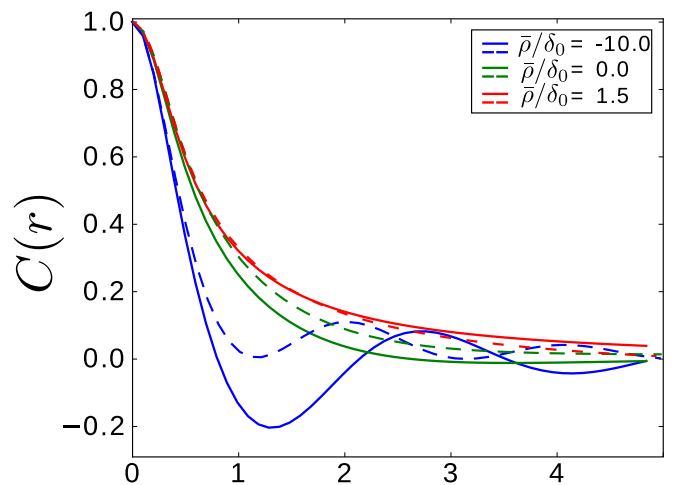


FIG. 3. Static spin-spin correlation function $C(r)$ in the spin-liquid phase for positive and negative spin stiffness ($b_2 = 0$, $\delta_0 \approx 0.04$). Solid lines correspond to the radius vector \mathbf{r} directed along the principal lattice axes (x or y), dashed lines correspond to \mathbf{r} along the diagonal direction.

keep higher-order terms $\mathcal{O}(q_i^6)$ in the expansion (2):

$$K(\mathbf{q}) = \rho q^2 + \frac{b}{2} q^4 + c(q_x^6 + q_y^6) + d(q_x^4 q_y^2 + q_x^2 q_y^4) \quad (29)$$

which break the symmetry with respect to spatial rotations in the $\{xy\}$ plane and remove the degeneracy with respect to the choice of the direction of \mathbf{Q} . After accounting for the higher-order anisotropic terms $\propto \mathcal{O}(q_i^6)$, the integral for $\langle \pi^2 \rangle$ becomes convergent at $|\mathbf{q}| = Q$ and the value ρ_{cS} is well defined.

V. SPIN-SPIN CORRELATION FUNCTION

Spin-spin correlations are a standard tool to analyze quantum critical properties of a magnetic system. In the SL phase the correlator provides essential information about the properties of the ground state. The equal-time two-point spin-spin correlation function reads as

$$C(r) = \langle n^\alpha(r) n^\alpha(0) \rangle = 1 + 2[R(r) - R(0)] + \dots, \quad (30)$$

where $\langle \pi^\alpha(r) \pi^\beta(0) \rangle = \delta^{\alpha\beta} R(r)$ and indices α, β refer only to the x and y spin components. The two-point correlator is normalized such that $C(0) = \langle n_\alpha^2 \rangle = 1$. In the SL phase the correlation function should vanish at large distances $C(r \rightarrow \infty) \rightarrow 0$ and $R(r \rightarrow \infty) \rightarrow 0$. These conditions are consistent with the ‘‘melting criterion’’ in Eq. (13) if we truncate the asymptotic expansion in Eq. (30), keeping only the terms explicitly presented there.

The $\langle \pi(r) \pi(0) \rangle$ correlation function in the SL phase reads as [18]

$$R(r) = \int \frac{i d\omega d^2q}{(2\pi)^3} \frac{e^{i\mathbf{q}\mathbf{r}}}{\chi_{\perp}(\omega^2 - \Delta^2) - K(\mathbf{q}) + i0}. \quad (31)$$

Calculating (31) and substituting the result in Eq. (30), we obtain the two-point spin-spin correlation function $C(r)$; the numerical results are plotted in Fig. 3. Similar to the previous section, these plots correspond to the case $b_2 = 0$. Therefore,

the correlator is somewhat anisotropic. There are two points to note, one is physical and another is technical. (i) The correlation length scales as one over the square root of the gap $\xi \propto 1/\sqrt{\delta_0}$, instead of the standard relation $\xi \propto 1/\delta_0$. (ii) When integrating in Eq. (31) we use the soft ultraviolet cutoff by multiplying the integrand by $e^{-q^2/(2\Lambda^2)}$. The soft cutoff allows us to avoid nonphysical oscillations in $R(r)$ due to the Gibbs phenomenon. The Gibbs phenomenon results in spurious oscillations, which always exist for a sharp cutoff and are well known in Fourier analysis.

The asymptotic behavior of the correlation function $R(r \rightarrow \infty)$ in the spin-liquid phase at $\rho = 0$ can be analytically obtained in the simplified isotropic approximation ($b_1 = b_2$):

$$R(r) \sim \frac{e^{-r\sqrt{\frac{\delta_0}{2}}}}{r} \cos\left(r\sqrt{\frac{\delta_0}{2}} - \frac{\pi}{4}\right). \quad (32)$$

Using Eq. (32) we deduce the spin-spin correlation length $\xi = \sqrt{\frac{2}{\delta_0}}$. In the case of negative spin stiffness ($\rho_{cS} < \rho < 0$) the correlation function $R(r)$ becomes oscillating (see Fig. 3). In the vicinity of the critical point ρ_{cN} the correlations decay as

$$R(r) = \frac{1}{2\pi\sqrt{2\chi_\perp b_1}} I_0\left(r\frac{\sqrt{\rho_{cN}}}{2}\right) K_0\left(r\frac{\sqrt{\rho_{cN}}}{2}\right) \underset{r \rightarrow \infty}{\sim} \frac{1}{r}. \quad (33)$$

Formula (33) is consistent with the well-known $\propto 1/r$ decay of correlations of transverse spin components in the Néel phase (see, e.g., Ref. [31]). We stress that the ‘‘isotropic approximation’’ $b_1 = b_2$ provides a qualitative and quantitative description of the correlation function $C(r)$ only away from the critical point ρ_{cS} . In the vicinity of the point ρ_{cS} the isotropic model (1) becomes unstable [see comments to Eq. (29)]. Deeply in Néel and spin-spiral phases the behavior of the correlator $C(r)$ at large distances, $r \rightarrow \infty$, is quite simple. In Néel phase the correlator becomes a constant $C(r) \rightarrow \langle n_z \rangle^2 \approx 1$, while in the spin-spiral phase there are nonvanishing oscillations $C(r) \rightarrow \cos Qr$ [18].

Now, we would like to make a comparison between $O(3)$ and $O(2)$ quantum Lifshitz transitions. The $O(2)$ version of Lagrangian (1) describes the XY frustrated Heisenberg antiferromagnet in the continuous limit. The physics in the $O(2)$ model is quite different from the $O(3)$ model and the Ioffe-Larkin argument is inapplicable in this case. The $O(2)$ Lagrangian can be mapped to the scalar Lifshitz model described by a polar angle θ : $n_x + in_y = e^{i\theta}$. This model has an exact solution for the correlation function $C(r)$ at the LP: $C(r)$ decays algebraically [32] at the LP in contrast to the nonvanishing correlations at $r \rightarrow \infty$ in long-range-ordered Néel or spin-spiral phase. Therefore, we conclude that there exists a finite region in the vicinity of the LP with algebraically decaying correlations. The region with algebraic spin correlations in some extent is analogous to the SL phase in the $O(3)$ model addressed in this paper.

VI. J_1 - J_3 MODEL ON THE SQUARE LATTICE

In this section we compare the field theory predictions with results of numerical calculations for the antiferromagnetic

J_1 - J_3 Heisenberg model on the square lattice. Frustrated J_1 - J_2 and J_1 - J_2 - J_3 models have been discussed in numerous studies (see, e.g., Refs. [4,6,33]): some references are also presented in the Introduction. In the classical limit, both models exhibit the spin-spiral state at a sufficiently large frustration. Quantum versions of the models show a magnetically disordered state at a sufficiently large frustration. Classically, the J_1 - J_2 model at $J_2/J_1 = \frac{1}{2}$ has three degenerate ground states: the Néel, the spin-spiral, and the spin stripe. The tricritical point is somewhat special; the proximity of the columnar spin stripe phase enhances spin-dimer correlations and makes the physics of the J_1 - J_2 model different from that considered in this work. On the other hand, if we set $J_2 = 0$ and consider only the J_3 frustration then classically there is a Lifshitz point with a transition to the spin spiral at $J_3 = J_1/4$, and the spin-stripe state has much higher energy than the spin-spiral and the Néel states. Therefore, the J_1 - J_3 model is a good testing ground for the generic theory of a Lifshitz transition developed in this work. The Hamiltonian of the J_1 - J_3 model reads as

$$H = J_1 \sum_{\langle ij \rangle} \mathbf{S}_i \mathbf{S}_j + J_3 \sum_{\langle\langle ij \rangle\rangle} \mathbf{S}_i \mathbf{S}_j, \quad (34)$$

where $\langle ij \rangle$ and $\langle\langle ij \rangle\rangle$ denote first- and third-nearest-neighbor interactions. The classical spin-spiral to Néel LP is located at $J_3/J_1 = \frac{1}{4}$. As we already pointed out in Sec. II, quantum fluctuations must shift the LP towards larger values $J_3/J_1 > \frac{1}{4}$.

In the long-wavelength approximation we can map the Heisenberg model to the Lagrangian (1). The magnetic susceptibility is well known:

$$\chi_\perp = \frac{1}{8J_1}. \quad (35)$$

The elasticity parameters of the Lagrangian can be found in two ways. (i) The first way is a straightforward expansion of the classical elastic energy at small wave number q , that gives

$$\rho = S^2(J_1 - 4J_3), \quad b_1 = S^2 \frac{(16J_3 - J_1)}{12}, \quad b_2 = 0. \quad (36)$$

(ii) An alternative way is to calculate the magnon dispersion in the Néel phase using the standard spin-wave theory. The dispersion reads as [4]

$$\omega_q = 4SJ_1 \sqrt{\left(1 - \frac{J_3}{J_1}(1 - \gamma_{2q})\right)^2 - \gamma_q^2}, \quad (37)$$

$$\gamma_q = \frac{1}{2}(\cos q_x + \cos q_y),$$

$$\gamma_{2q} = \frac{1}{2}(\cos 2q_x + \cos 2q_y). \quad (38)$$

Expanding ω_q at small q and comparing the results with Eq. (8) (at $\Delta = 0$) we find

$$\rho = S^2(J_1 - 4J_3),$$

$$b_1 = 4J_1 S^2 \left[-\frac{5}{48} + \frac{2}{3} \left(\frac{J_3}{J_1} \right) + \left(\frac{J_3}{J_1} \right)^2 \right],$$

$$b_2 = 4J_1 S^2 \left[-\frac{1}{8} + 2 \left(\frac{J_3}{J_1} \right)^2 \right]. \quad (39)$$

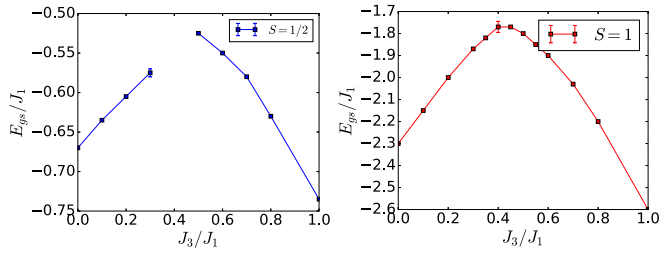


FIG. 4. J_1 - J_3 model ground-state energy in the Néel and in the spin-spiral states for (a) $S = \frac{1}{2}$ and (b) $S = 1$ calculated by numerical series expansion method.

Expressions for b_1 and b_2 in Eqs. (36) and (39) do not coincide. At the LP, $J_3 = J_1/4$, both equations give $b_2 = 0$, however, values of b_1 are different, Eq. (36) gives $b_1 = 0.25S^2J_1$, while Eq. (39) gives $b_1 = 0.5S^2J_1$. Of course, the spin-wave theory value is more reliable.

We have performed extensive series calculations both in the Néel phase and the spin-spiral phase. Unfortunately, the series expansion method does not allow to assess properties of the spin-liquid phase directly. However, it allows to estimate the range of parameters where the spin liquid exists which can be compared with predictions of the field theory. In the Néel phase, the series starts from the simple Ising antiferromagnetic state. In the spiral phase, the calculation is more tricky. We first impose a classical diagonal spiral with some wave vector Q and find the total energy of this state $E(Q)$. This includes the classical energy and the quantum corrections calculated by means of series expansions. We perform this calculation for many values of Q and then find numerically the minimum of $E(Q)$. Such procedure gives us the ground-state energy E_{gs} and the physical wave vector Q . The ground-state energy E_{gs} is plotted in Fig. 4 versus J_3 . The plot of the wave vector squared Q^2 versus J_3 is presented in Fig. 5. From the field-theory description we expect that near the LP the wave

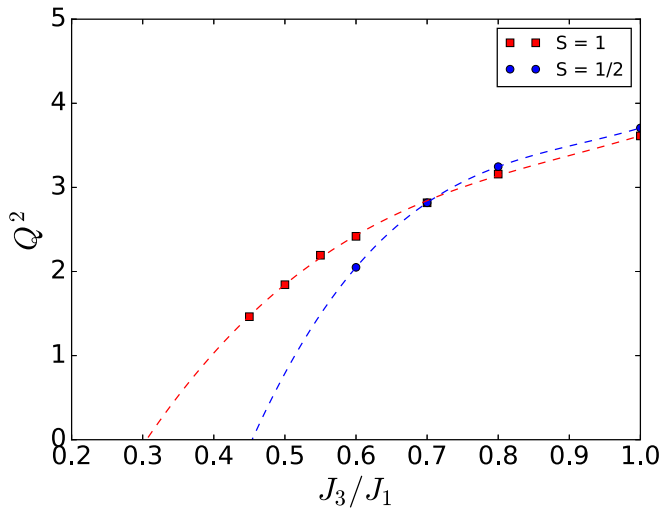


FIG. 5. Spiral wave vector (squared) Q^2 versus J_3 . Dots show results of numerical series expansion. Red dots correspond $S = \frac{1}{2}$ ($S = 1$). Dashed lines show fits of data by cubic polynomials $Q^2 = a_1(J_3 - J_3^{LP}) + a_2(J_3 - J_3^{LP})^2 + a_3(J_3 - J_3^{LP})^3$.

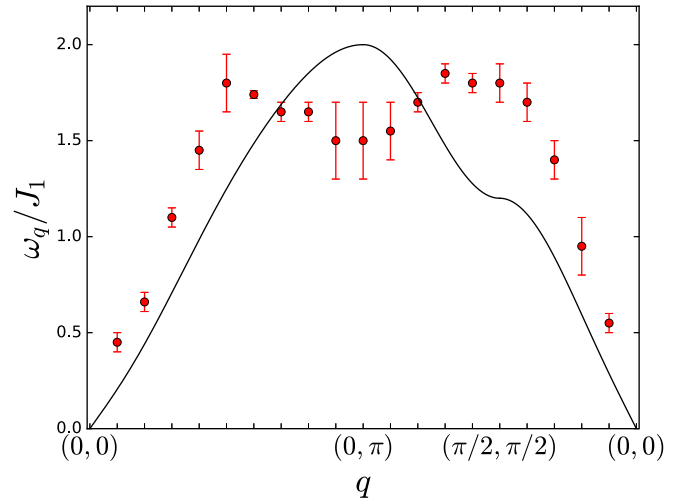


FIG. 6. Magnon dispersion ω_q for J_1 - J_3 model on the square lattice in the Néel phase at $J_3/J_1 = 0.2$. Red circles correspond to the series expansion results, black line is the linear spin-wave dispersion in Eq. (37).

vector behaves as

$$Q^2 = \frac{2|\rho|}{b_1} = \frac{8S^2}{b_1}(J_3 - J_3^{LP}). \quad (40)$$

Therefore, from Fig. 5 we determine positions of Lifshitz points and, using Eq. (40) we find the values of the elastic constant b_1 at the LP:

$$\begin{aligned} S = 1/2 : \quad J_3^{LP} &\approx 0.45J_1, \quad b_1/S^2 \approx 0.60J_1, \\ S = 1 : \quad J_3^{LP} &\approx 0.3J_1, \quad b_1/S^2 \approx 0.74J_1. \end{aligned} \quad (41)$$

As expected (see the very end of Sec. II), quantum fluctuations extend the Néel phase in relation to the classical LP $J_3^{LP} = 0.25J_1$. Values of the elastic constant b_1 are larger than that given by Eqs. (36) and (39). This is not very surprising having in mind that the LP location is different from its classical value.

We have also calculated the magnon dispersion in the Néel phase. The series expansion becomes erratic at $J_3 > 0.2J_1$ and the error bars in the calculations of ω_q grow very quickly. The dispersion at $J_3 = 0.2J_1$ is shown in Fig. 6. We see that the shape of the dispersion is somewhat different from the prediction of the spin-wave theory (37). On the other hand, the total bandwidth is consistent with the spin-wave theory. The situation is different in the case of a simple Heisenberg model ($J_3 = 0$), when the shape of magnon dispersion is consistent with the spin-wave theory but the total bandwidth is about 20% larger compared to the spin-wave theory value.

We also compute the static onsite magnetization in the Néel and spiral phases. The magnetization vanishes at J_3^{cN} and J_3^{cS} critical points. We already pointed out that the Néel-SL transition at J_3^{cN} belongs to the $O(3)$ universality class. Therefore, we expect scaling $\langle S_z \rangle \propto |J_3 - J_3^{cN}|^\beta$ when approaching the critical point from the Néel phase, here $\beta = (D - 2 + \eta)v/2 \approx v/2 \approx 0.35$ [18]. Due to this reason in Fig. 7 we show series expansion results for the static onsite

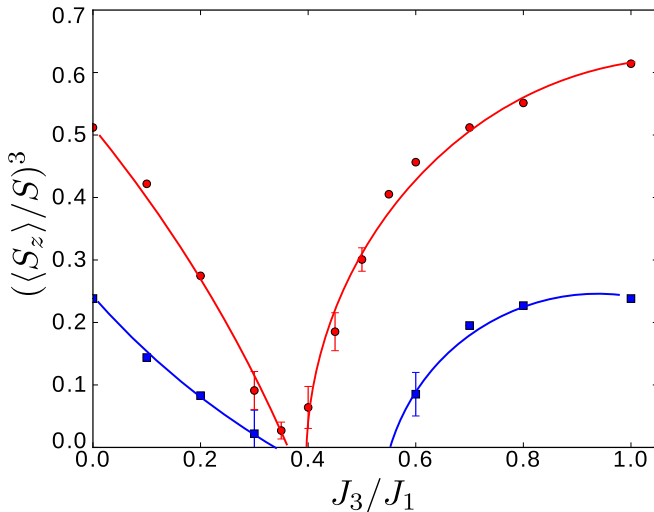


FIG. 7. Average onsite magnetization cubed. Blue squares (red circles) show series expansion results for $S = \frac{1}{2}$ ($S = 1$), solid lines are guides for the eye.

magnetization cubed. From here we locate the critical points:

$$\begin{aligned} S = 1/2 : \quad J_3^{cN} &\approx 0.35J_1, \quad J_3^{cS} \approx 0.55J_1, \\ S = 1 : \quad J_3^{cN} &\approx J_3^{cS} \approx 0.35J_1. \end{aligned} \quad (42)$$

Our result for the SL range ΔJ_3 in the case $S = \frac{1}{2}$ is different from the recent work [6], that suggests the SL phase at $0.4 \leq J_3/J_1 \leq 0.8$. However, our predictions are reasonably close to the exact diagonalization results [33], suggesting the gapped SL phase for $0.45 \leq J_3/J_1 \leq 0.65$. Note also that the critical index for the the J_3^{cS} critical point is smaller than the $O(3)$ value, $M \propto (J_3 - J_3^{cS})^\beta$, $\beta \sim 0.2$.

Now, we can compare the results of series calculations with predictions of the field theory. Equations (35) and (41) give values of χ_\perp and b_1 . Hence, according to Eqs. (19) and (16), values of the gap at the LP are

$$\begin{aligned} S = 1/2 : \quad \delta_0 &\approx 0.66, \quad \Delta_0 \approx 0.53J_1, \\ S = 1 : \quad \delta_0 &\approx 0.17, \quad \Delta_0 \approx 0.29J_1. \end{aligned} \quad (43)$$

Formally, the field-theoretical prediction (16) is derived within logarithmic accuracy and valid at $\delta_0 \ll 1$, while these values, especially that at $S = \frac{1}{2}$, are not small. Nevertheless, we believe that Eq. (43) gives a reasonable estimate of the gaps. Knowing the dimensionless gaps and using Fig. 2 we can deduce the window $\delta\bar{\rho}$ occupied by the spin-liquid phase. Combining this with Eq. (40), we find the spin-liquid window $\Delta J_3 = |J_3^{cS} - J_3^{cN}|$ that follows from the field theory

$$\begin{aligned} \Delta J_3/J_1 &\approx 0.3 \quad (S = 1/2), \\ \Delta J_3/J_1 &\approx 0.1 \quad (S = 1). \end{aligned} \quad (44)$$

These values, while being slightly larger, are in a reasonable agreement with the SL phase windows following from series expansion data in Fig. 7.

In conclusion of this section, we would like to comment on the anisotropic J_1 - J_3 model on square lattice [11]. In this model, J_3 frustrates J_1 only in one direction, say J_3 connects only the third-nearest neighbors in the y direction. This results

in an anisotropic LP: the spin stiffness ρ_y vanishes at some value of J_3 while ρ_x remains finite and positive. The wave vector of the spin spiral is always directed along the y axis. In this case, quantum fluctuations at the LP are described as $\langle \pi^2 \rangle \propto \int \frac{d^2q}{\sqrt{q_x^2 + q_y^2 + \rho_x q_x^2}}$. The integral is infrared convergent unlike that in the isotropic LP. Therefore, generically one cannot expect a spin liquid in this case. The fluctuations are still enhanced and there must be a suppression of the onsite magnetization at the LP. This is exactly what series expansions for the anisotropic J_1 - J_3 model with $S = \frac{1}{2}$ indicate [11]. The suppression of the local onsite magnetization has been observed in antiferromagnetic compound CaMn_2Sb_2 which consists of weakly coupled hexagonal layers [14]. This material accidentally lies very close to a Néel-spiral LP. Unfortunately, a formation of a true spin liquid in this compound is prevented due to a large value of spin. The large spin results in two effects [14]: (i) it suppresses quantum fluctuations at LP and (ii) it creates an easy-axis spin anisotropy that breaks $O(3)$ rotational invariance and opens a small magnetic gap. SL phase can be potentially observed in future experiments in similar compounds when substituting Mn with a large spin by a magnetic element with a smaller spin.

It is likely that a similar scenario is valid for thin films of frustrated manganites $(\text{Tb,La,Dy})\text{MnO}_3$ tuned close to LP. In fact, the in-plane Heisenberg interactions in manganites are somewhat anisotropic by analogy with the anisotropic J_1 - J_3 model discussed above. This anisotropy results in different values of the spin stiffness $\rho_{x,y}$ along x, y axes. The suppression of the onsite magnetization at the LP can be observed in thin films of manganates in elastic neutron scattering experiments.

VII. DISCUSSION AND CONCLUSIONS

In this work, using field-theory techniques, we have studied properties of the universal spin-liquid phase in a vicinity of an isotropic Lifshitz point in a system of localized frustrated spins. Our general analysis includes the phase diagram, positions of critical points, excitation spectra, and spin-spin correlation functions. In the semiclassical regime of large spin S the spin-liquid phase forms an exponentially narrow region in the vicinity of the Lifshitz point. The derivation of these results is accompanied with a thorough discussion of the criterion for quantum melting of long-range magnetic order in two dimensions, an analog of Lindemann criterion. We argue the 2D Lifshitz point spin liquid is similar to the gapped Haldane phase in integer-spin 1D chains. The quasiparticle excitations in the SL phase are threefold degenerate due to unbroken $O(3)$ rotational symmetry and hence have spin 1. In order to check our general field-theory results, and in particular to check the quantum melting criterion, we have performed numerical series expansion calculations for the J_1 - J_3 model on the square lattice. We demonstrate that results of these two different approaches are in a good agreement. Last but not least, the field-theoretical approach developed in this work can be applied to systems which consist of both localized and itinerant electrons, in particular the t - J model and cuprate superconductors [34].

ACKNOWLEDGMENTS

We would like to thank G. Khaliullin for insightful comments and suggestions. The work has been supported by Australian Research Council Grant No. DP160103630.

APPENDIX A: THE VALUE OF $\langle \pi^2 \rangle_c$ DERIVED FROM ASYMPTOTIC TAYLOR EXPANSION

After expanding $n_z = \sqrt{1 - \pi^2}$ in a Taylor series and using Wick's theorem,

$$\begin{aligned} \langle n_z \rangle &= 1 - \sum_{k=1}^{\infty} \langle \pi^2 \rangle^k \frac{(2k-2)!}{2^{2k-1}(k-1)!} \\ &= 1 - \frac{1}{2} \langle \pi^2 \rangle - \frac{1}{4} \langle \pi^2 \rangle^2 - \frac{3}{8} \langle \pi^2 \rangle^3 + \dots \end{aligned} \quad (\text{A1})$$

The series (A1) is asymptotic and the coefficients at large k diverge. Since the series is asymptotic, we truncate it when the coefficients in front of $\langle \pi^2 \rangle^k$ terms become larger than unity. Accounting for the leading terms in the expansion up to $\langle \pi^2 \rangle^3$ inclusive gives the critical value $\langle \pi^2 \rangle_c \approx 0.93$ for $\langle n_z \rangle = 0$.

APPENDIX B: EXCITATIONS IN STATIC SPIN-SPIRAL PHASE

By considering fluctuations in the spin-spiral state we find the condition when quantum fluctuations melt the spiral. Here, we derive the dispersions of in-plane and out-of-plane fluctuations in the spin-spiral state. To be specific, let us assume that the spiral lies in $\{xy\}$ plane:

$$\mathbf{n} = (\cos \mathbf{Q}\mathbf{r}, \sin \mathbf{Q}\mathbf{r}, 0). \quad (\text{B1})$$

There are two different spin waves, the in-plane $\varphi(\mathbf{r}, t)$,

$$\mathbf{n} = (\cos(\mathbf{Q}\mathbf{r} + \phi), \sin(\mathbf{Q}\mathbf{r} + \phi), 0), \quad (\text{B2})$$

and the out-of-plane $h(\mathbf{r}, t)$,

$$\mathbf{n} = (\sqrt{1-h^2} \cos \mathbf{Q}\mathbf{r}, \sqrt{1-h^2} \sin \mathbf{Q}\mathbf{r}, h). \quad (\text{B3})$$

Substituting parametrization (B2) and (B3) in the Euler-Lagrange equations of motion corresponding to the Lagrangian (1) and linearizing the equations with respect to ϕ and h we obtain the dispersion of the in-plane and out-of-plane modes. The derivation is straightforward (see, e.g., Ref. [15]). The dispersion of the in-plane mode is

$$\begin{aligned} \omega_q^2 &= \frac{1}{\chi_{\perp}} \left[K(\mathbf{Q}) - \frac{1}{2} [K(\mathbf{Q} + \mathbf{q}) + K(\mathbf{Q} - \mathbf{q})] \right] \\ &= \frac{b_1}{2\chi_{\perp}} [2Q^2 q^2 + q_x^4 + q_y^4], \end{aligned} \quad (\text{B4})$$

and the dispersion of the out-of-plane mode is

$$\begin{aligned} \Omega_q^2 &= \frac{1}{\chi_{\perp}} [K(\mathbf{q}) - K(\mathbf{Q})] \\ &= \frac{b_1}{2\chi_{\perp}} [Q^4/2 - Q^2 q^2 + q_x^4 + q_y^4]. \end{aligned} \quad (\text{B5})$$

The total quantum fluctuation orthogonal to the spin alignment in the spiral phase reads as

$$\begin{aligned} \langle \pi^2 \rangle &= \langle \phi^2 \rangle + \langle h^2 \rangle, \\ \langle \phi^2 \rangle &= \int \frac{d^2 q}{(2\pi)^2} \frac{1}{2\omega_q}, \\ \langle h^2 \rangle &= \int \frac{d^2 q}{(2\pi)^2} \frac{1}{2\Omega_q}. \end{aligned} \quad (\text{B6})$$

From the condition $\langle \pi^2 \rangle = \langle \pi^2 \rangle_c \approx 1$ we find the position of the spiral-SL critical point ρ_{cS} (see Sec. IV in the main text).

-
- [1] L. Savary and L. Balents, *Rep. Prog. Phys.* **80**, 016502 (2017).
[2] L. Balents and O. A. Starykh, *Phys. Rev. Lett.* **116**, 177201 (2016).
[3] L. B. Ioffe and A. I. Larkin, *J. Mod. Phys. B* **2**, 203 (1988).
[4] J. Ferrer, *Phys. Rev. B* **47**, 8769 (1993).
[5] L. Capriotti, D. J. Scalapino, and S. R. White, *Phys. Rev. Lett.* **93**, 177004 (2004).
[6] J. Reuther, P. Wölfle, R. Darradi, W. Brenig, M. Arlego, and J. Richter, *Phys. Rev. B* **83**, 064416 (2011).
[7] J. Reuther, D. A. Abanin, and R. Thomale, *Phys. Rev. B* **84**, 014417 (2011).
[8] Z. Zhu, D. A. Huse, and S. R. White, *Phys. Rev. Lett.* **110**, 127205 (2013).
[9] H. Zhang and C. A. Lamas, *Phys. Rev. B* **87**, 024415 (2013).
[10] R. F. Bishop, P. H. Y. Li, O. Götze, J. Richter, and C. E. Campbell, *Phys. Rev. B* **92**, 224434 (2015).
[11] J. Oitmaa and R. P. Singh, *Phys. Rev. B* **94**, 214430 (2016).
[12] J. Merino and A. Ralko, *Phys. Rev. B* **97**, 205112 (2018).
[13] F. D. M. Haldane, *Phys. Rev. Lett.* **50**, 1153 (1983).
[14] D. E. McNally, J. W. Simonson, J. J. Kistner-Morris, G. J. Smith, J. E. Hassinger, L. DeBeer-Schmitt, A. I. Kolesnikov, I. A. Zaliznyak, and M. C. Aronson, *Phys. Rev. B* **91**, 180407(R) (2015).
[15] A. I. Milstein and O. P. Sushkov, *Phys. Rev. B* **91**, 094417 (2015).
[16] D. Bergman, J. Alicea, E. Gull, S. Trebst, and L. Balents, *Nat. Phys.* **3**, 487 (2007).
[17] A. M. Polyakov, *Phys. Lett. B* **59**, 79 (1975).
[18] S. Sachdev, *Quantum Phase Transitions* (Cambridge University Press, Cambridge, 1999).
[19] P. Azaria, B. Delamotte, and T. Jolicoeur, *Phys. Rev. Lett.* **64**, 3175 (1990).
[20] N. Read and S. Sachdev, *Phys. Rev. B* **42**, 4568 (1990).
[21] A. Chubukov, S. Sachdev, and T. Senthil, *Nucl. Phys. B* **426**, 601 (1994).
[22] I. Affleck, *J. Phys.: Condens. Matter* **1**, 3047 (1989).
[23] C. Kittel, *Quantum Theory of Solids* (Wiley, New York, 1963).
[24] F. A. Lindemann, *Phys. Z.* **11**, 609 (1910).
[25] J.-P. Renard, L.-P. Regnault, and M. Verdaguer, *Magnetism: Molecules to Materials I: Models and Experiments*, edited by J. S. Miller and M. Drillon (Wiley-VCH, Weinheim, Germany, 2003), Chap. 2, pp. 49–93.
[26] E. H. Lieb, T. D. Schultz, and D. C. Mattis, *Ann. Phys. (NY)* **16**, 407 (1961).
[27] M. B. Hastings, *Phys. Rev. B* **69**, 104431 (2004).

- [28] S. Takayoshi, P. Pujol, and A. Tanaka, *Phys. Rev. B* **94**, 235159 (2016).
- [29] Y. A. Kharkov, O. P. Sushkov, and M. Mostovoy, *Phys. Rev. Lett.* **119**, 207201 (2017).
- [30] P. V. Shevchenko, A. W. Sandvik, and O. P. Sushkov, *Phys. Rev. B* **61**, 3475 (2000).
- [31] M. Takahashi, *Phys. Rev. B* **40**, 2494 (1989).
- [32] E. Ardonne, P. Fendley, and E. Fradkin, *Ann. Phys. (NY)* **310**, 493 (2004).
- [33] P. Sindzingre, N. Shannon, and T. Momoi, *J. Phys.: Conf. Ser.* **200**, 022058 (2010).
- [34] Y. A. Kharkov and O. P. Sushkov, *Phys. Rev. B* **98**, 155118 (2018).